DENSE BARYONIC MATTER*

Peter Senger

Gesellschaft für Schwerionenforschung (GSI)
Postfach 110552, 64220 Darmstadt, Germany

(Received December 1, 2005)

Experiments on strangeness production in nucleus–nucleus collisions at SIS energies address fundamental aspects of modern nuclear physics: the determination of the nuclear equation-of-state at high baryon densities and the properties of hadrons in dense nuclear matter. Experimental data and theoretical results will be reviewed. Future experiments at the FAIR accelerator aim at the exploration of the QCD phase diagram at highest baryon densities. The proposal for the Compressed Baryonic Matter (CBM) experiment will be presented.

PACS numbers: 25.75.Dw

1. Introduction

High-energy heavy-ion collision experiments offer the unique possibility to create and investigate extreme states of strongly-interacting matter in the laboratory. The aim of these experiments is to obtain information on *(i)* the properties of hadrons in dense or hot baryonic/hadronic matter, *(ii)* the restoration of chiral symmetry at high temperatures and high baryon densities, *(iii)* the deconfinement phase transition from hadronic to quark–gluon matter at high temperatures and/or high baryon densities, and *(iv)* the nuclear equation-of-state at high baryon densities. These issues are related to fundamental aspects of strong interaction physics and its underlying theory, quantum chromodynamics (QCD), and are also of great importance for our understanding of astrophysical phenomena like supernova dynamics and the stability of neutron stars [1, 2].

* Presented at the XXIX Mazurian Lakes Conference on Physics August 30–September 6, 2005, Piaski, Poland.

2. Strangeness production at threshold beam energies

The study of strangeness production in heavy-ion collisions addresses basic questions in nuclear physics such as the equation of state at high baryon densities and the modification of hadron properties in dense and hot hadronic or baryonic matter. Corresponding experiments on kaon and antikaon production and propagation in heavy-ion collisions at SIS energies have been performed with the Kaon Spectrometer and the FOPI detector at SIS/GSI. The most important results are published in [3–10].

2.1. The nuclear equation-of-state

K^+ mesons have been proposed already many years ago as a promising diagnostic probe for the nuclear equation-of-state. Microscopic transport calculations indicate that the yield of kaons created in collisions between heavy nuclei at subthreshold beam energies ($E_{\mathrm{beam}} = 1.58\,\mathrm{GeV}$ for $NN \to K^+\Lambda N$) is sensitive to the compressibility of nuclear matter at high baryon densities [11, 12]. This sensitivity is due to the production mechanism of K^+ mesons. At subthreshold beam energies, the production of kaons requires multiple nucleon–nucleon collisions or secondary collisions such as $\pi N \to K^+\Lambda$. These processes are expected to occur predominantly at high baryon densities, and the densities reached in the fireball depend on the nuclear equation-of-state [13]. According to transport calculations, in central Au+Au collisions the bulk of K^+ mesons is produced at nuclear matter densities larger than twice saturation density.

Moreover, K^+ mesons are well suited to probe the properties of the dense nuclear medium because of their long mean free path. The propagation of K^+ mesons in nuclear matter is characterized by the absence of absorption (as they contain an antistrange quark) and hence kaons emerge as messengers from the dense phase of the collision. In contrast, the pions created in the high density phase of the collision are likely to be reabsorbed and most of them will leave the reaction zone in the late phase.

The influence of the medium on the K^+ yield is amplified by the steep excitation function of kaon production near threshold energies. Early transport calculations find that the K^+ yield from Au+Au collisions at subthreshold energies will be enhanced by a factor of about 2 if a soft rather than a hard equation-of-state is assumed [11, 12]. Recent calculations take into account the modification of the kaon properties in the dense nuclear medium [14, 15] (see next chapter). When assuming a repulsive K^+N potential as proposed by various theoretical models (see [16] and references therein) the energy needed to create a K^+ meson in the nuclear medium is increased and hence the K^+ yield will be reduced. Therefore, the yield of K^+ mesons produced in heavy ion collisions is affected by both the nuclear compressibility and the in-medium kaon potential.

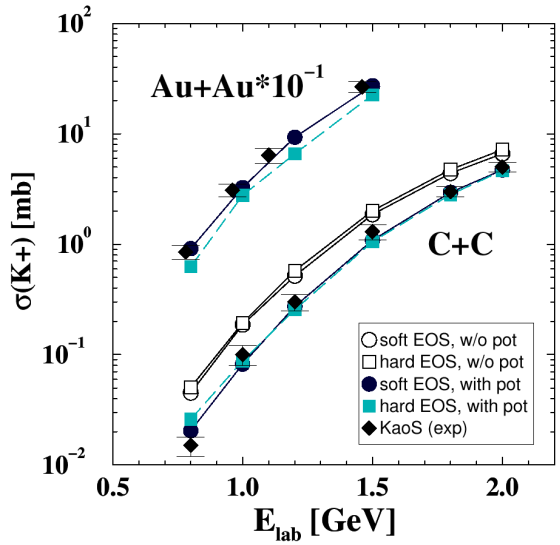

Fig. 1. Production cross sections of K^+ mesons for Au+Au and C+C collisions as a function of the projectile energy per nucleon. The data (full diamonds) are compared to results of transport calculations assuming a soft (circles) and a hard (squares) nuclear equation-of-state with and without K^+N in-medium potentials. Taken from [17].

The KaoS Collaboration proposed to disentangle these two competing effects by studying K^+ production in a very light (^{12}C+^{12}C) and a heavy collision system (^{197}Au+^{197}Au) at different beam energies near threshold [8]. The reaction volume is more than 15 times larger in Au+Au than in C+C collisions and hence the average baryonic density, achieved by the pile-up of nucleons, is significantly higher [15]. Moreover, the maximum baryonic density reached in Au+Au collisions depends on the nuclear compressibility [12,18] whereas in the small C+C system this dependence is very weak [19].

Recent QMD transport calculations which take into account a repulsive kaon–nucleon potential reproduce the energy dependence of the kaon ratio if a compression modulus of $\kappa = 200\,\mathrm{MeV}$ for nuclear matter is assumed [19]. These calculations use momentum-dependent Skyrme forces to determine the compressional energy per nucleon (*i.e.* the energy stored in compression) as function of nuclear density. The result of this calculation is presented in Fig. 1 in comparison with the data [8].

In order to reduce systematic uncertainties both in experiment (normalization, efficiencies, acceptances *etc.*) and theory (elementary cross sections *etc.*) the K^+ multiplicities are plotted as ratios $(K^+/A)_{\mathrm{Au+Au}}$ / $(K^+/A)_{\mathrm{C+C}}$ in Fig. 2. In this representation also the in-medium effects

cancel to a large extent. The calculations are performed with a compression modulus of $\kappa = 380\,\mathrm{MeV}$ (a "hard" equation-of-state) and with $\kappa = 200\,\mathrm{MeV}$ (a "soft" equation-of-state) [17, 19]. The data clearly favor a soft equation-of-state (see Fig. 2).

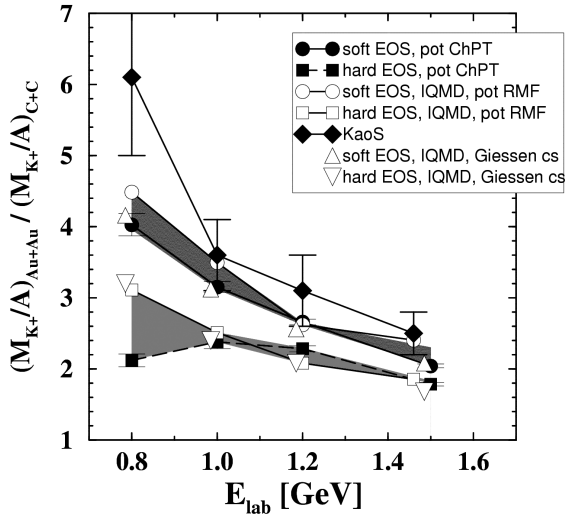

Fig. 2. K^+ ratio measured in inclusive Au+Au and C+C collisions as function of beam energy [8]. The data are compared to various QMD calculations assuming nuclear compressibilities of $\kappa = 200\,\mathrm{MeV}$ and 380 MeV. Taken from [17].

2.2. In-medium properties of kaons and antikaons

According to various calculations, the properties of kaons and antikaons are modified in dense baryonic matter (see *e.g.* [15, 16, 20]). In mean-field calculations, this effect is caused by a repulsive K^+N potential and an attractive K^-N potential. It has been speculated that an attractive K^-N potential will lead to Bose condensation of K^- mesons in the core of neutron stars above baryon densities of about 3 times saturation density [21].

Fig. 3 illustrates the dependence of the kaon and antikaon total energy on the nuclear density according to various calculations. The compilation of theoretical results is taken from [16]. The calculations have been performed with a relativistic mean-field model (RMF), chiral perturbation theory (ChPT) and a coupled channel code [22]. All models exhibit quite similar features: the kaon energy increases and the antikaon energy decreases with increasing density. The parameterizations shown in Fig. 3 are used in transport model simulations of heavy ion collisions (see *e.g.* [15, 16, 20]).

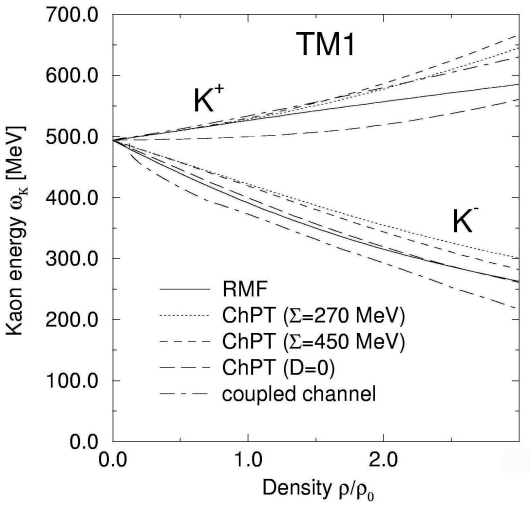

Fig. 3. The total energy of kaons and antikaons (at rest) in nuclear matter as a function of density for a soft equation-of-state. The curves are calculated with a relativistic mean-field model (RMF), chiral perturbation theory (ChPT with different Σ terms) and a coupled-channel code (taken from [16]).

A comparison of experimental data to results of various transport model calculations is presented in Fig. 4. The figure shows the K^+ multiplicity densities dN/dy for near-central Ni+Ni collisions at 1.93 AGeV as function of the c.m. rapidity. Fig. 4 combines data measured by the KaoS Collaboration [7] and by the FOPI Collaboration [3,23]. The transport calculations clearly disagree with the data if in-medium effects are neglected (open symbols). However, when taking into account a repulsive K^+N potential, the K^+ yield is reduced, and the calculations agree with the data sufficiently well (full symbols).

Another observable consequence of in-medium KN potentials is their influence on the propagation of kaons and antikaons in heavy-ion collisions. The measured azimuthal emission patterns of K^+ mesons contradict the expectations based on a long mean free path in nuclear matter. The particular feature of sideward flow [6] and the pronounced out-of-plane emission around midrapidity [4] indicate that K^+ mesons are repelled from the regions of increased baryonic density as expected for a repulsive K^+N potential [24,25].

Fig. 5 depicts the azimuthal angle distributions of K^+ mesons measured in Au+Au collisions at 1.0 AGeV (left panel) and in Ni+Ni collisions at a beam energy of 1.93 AGeV (right panel). The K^+ emission patterns clearly are peaked at $\phi = \pm 90°$ which is perpendicular to the reaction plane. Such a behavior is known from pions which are shadowed by the spectator fragments. In the case of K^+ mesons, however, the anisotropy can be explained

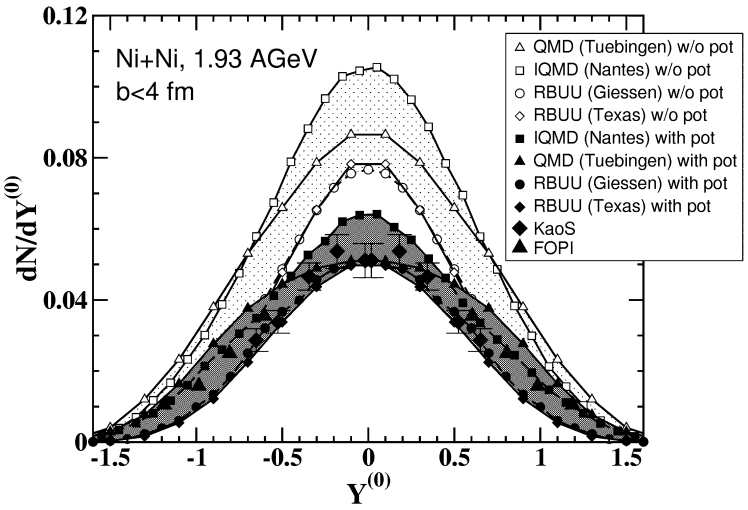

Fig. 4. Multiplicity density distributions of K^+ mesons for near-central ($b < 4.4$ fm) Ni+Ni collisions at 1.93 AGeV. Full black diamonds: KaoS data [7], full black triangles: FOPI data [3,23]. The data are compared to various transport calculations. Full symbols: with in-medium effects. Open symbols: without in-medium effects. Taken from [17].

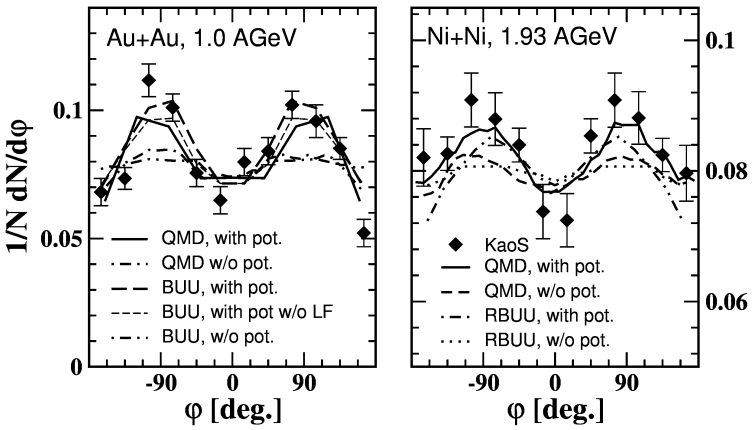

Fig. 5. K^+ azimuthal distributions for semi-central Au+Au at 1 AGeV (left panel) and for Ni+Ni collisions at 1.93 AGeV (right panel). The data (full symbols) are compared to various transport calculations with and without in-medium potentials (see insert). Taken from [17], see also [26].

by transport calculations only if a repulsive in-medium K^+N potential is assumed. A flat distribution is expected when neglecting the in-medium potential [17, 26].

The key observable for the K^-N in-medium potential is the azimuthal emission pattern of K^- mesons. The existence of an attractive K^-N potential will strongly reduce the absorption of K^- mesons, and consequently the K^- mesons will be emitted almost isotropically in semicentral Au+Au collisions [25]. This observation would be in contrast to the behavior of pions and K^+ mesons, and would provide strong experimental evidence for in-medium modifications of antikaons. Fig. 6 depicts the first data on the K^- azimuthal emission pattern measured in heavy-ion collisions (lower panel) which differs significantly from the corresponding K^+ pattern (upper panel) [10]. The lines refer to results of IQMD calculations with and without in-medium potentials for K^+ and K^- mesons [27]. Further clarification will come from high statistics data which have been measured in Au+Au collisions at 1.5 AGeV, and which are presently being analyzed.

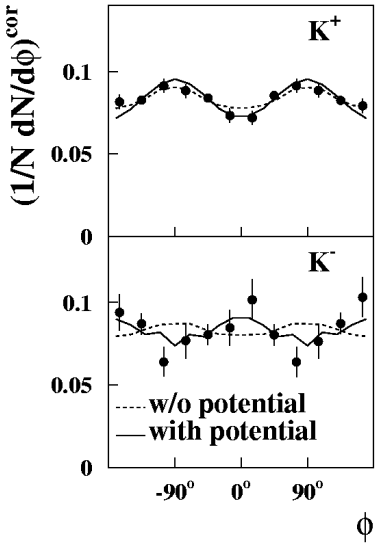

Fig. 6. K^+ and K^- azimuthal distribution for semi-central Ni+Ni collisions at 1.93 AGeV [10]. The data are corrected for the resolution of the reaction plane and refer to impact parameters of 3.8 fm $< b <$ 6.5 fm, rapidities of $0.3 < y/y_{\mathrm{beam}} < 0.7$ and momenta of $0.2\,\mathrm{GeV}/c < p_{\mathrm{t}} < 0.8\,\mathrm{GeV}/c$ [10]. The lines represent results of transport calculations from the Nantes group using a IQMD model [27]. Solid lines: with in-medium KN potential. Dashed lines: without in-medium KN potential.

In the mean field calculations as discussed above the K^- mesons are treated as quasi-particles which are on the mass shell. Microscopic coupled-channel calculations based on a chiral Lagrangian, however, predict a dynamical broadening of the K^- meson spectral function in dense nuclear matter [22, 28]. First off-shell transport calculations using K^- meson spectral functions have been performed [29]. The ultimate goal of the calculations is to relate the in-medium spectral function of K^- mesons to the anticipated chiral symmetry restoration at high baryon density. New experimental information on the in-medium modification of vector mesons is expected from the dilepton experiments with HADES at GSI. Highest baryon densities will be produced and explored with the Compressed Baryonic Matter (CBM) experiment at the future FAIR accelerator center in Darmstadt.

3. CBM at FAIR: Towards highest baryon densities

The future international Facility for Antiproton and Ion Research (FAIR) in Darmstadt will provide unique research opportunities in the fields of nuclear, hadron, atomic and plasma physics [30]. The accelerators will deliver primary beams (protons up to 90 GeV, Uranium up to 35 AGeV, nuclei with $Z/A = 0.5$ up to 45 AGeV) and secondary beams (rare isotopes and antiprotons) with high intensity and quality. The aim of the nucleus–nucleus collision research program is to explore the QCD phase diagram at high net baryon densities and moderate temperatures. This approach is complementary to the studies of matter at high temperatures and low net baryon densities performed at RHIC and LHC. At high baryon densities, new phases of strongly interacting matter are expected [1, 2, 31]. This exciting new field of high baryon density QCD needs input from experimental data, which can only be provided by new and dedicated nucleus–nucleus collision experiments.

The phase boundary between quark–gluon matter and hadronic matter has been studied recently by lattice QCD calculations [32, 33]. The calculations predict a critical endpoint at a temperature of $T \approx 160$ MeV and a baryon chemical potential $\mu_B \approx 400$ MeV, indicating a first order phase transition above $\mu_B \approx 400$ MeV, and a smooth cross over from hadronic to partonic matter below this value. The search for the critical endpoint is a prime goal of high-energy heavy-ion collision experiments.

Trajectories of nucleus–nucleus collisions in the T–μ_B plane have been recently calculated with a 3-fluid hydrodynamics model [34]. Fig. 7 depicts the trajectories corresponding to different beam energies. According to the calculations a beam energy of 10 AGeV is sufficient to cross the phase boundary. A beam energy of about 30 AGeV is suggested to search for the critical endpoint.

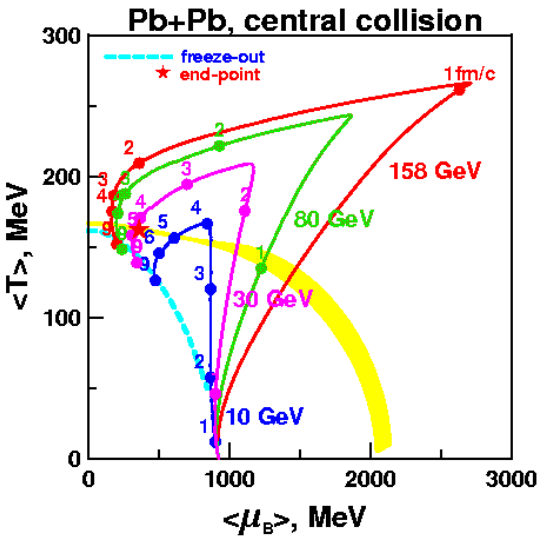

Fig. 7. Trajectories of heavy ion collisions in the QCD phase diagram calculated by a 3-fluid hydrodynamics model [34]. Dashed line: chemical freeze-out curve. Star: critical endpoint.

3.1. Observables

The major challenge is to find diagnostic probes which are connected to the onset of chiral symmetry restoration, to the deconfinement phase transition, and to the equation-of-state of hadronic and partonic matter.

The in-medium spectral functions of short-lived vector mesons, which are expected to be sensitive to chiral symmetry restoration, can be studied in the dense nuclear medium via their decay into lepton pairs [35]. Since the leptons are very little affected by the passage through the high-density matter, they provide, as a penetrating probe, almost undistorted information on the conditions in the interior of the collision zone. Another observable sensitive to in-medium effects is open charm, *e.g.* D-mesons. The effective masses of D-mesons, a bound state of a heavy charm quark and a light quark, are expected to be modified in dense matter similarly to those of kaons. Such a change would be reflected in the relative abundance of charmonium ($c\bar{c}$) and D-mesons.

The onset of a first order phase transition is expected to cause discontinuities in sensitive observables when varying the beam energy in relativistic nucleus–nucleus collisions. Such a non-monotonic behavior has been observed around 30 AGeV in the kaon-to-pion ratio and in the inverse slope parameter of kaons [36]. A beam energy scan looking at a variety of ob-

servables is needed to clarify the experimental situation. This includes the measurement of the phase-space distributions of strange particles, in particular multi-strange baryons (antibaryons), and particles containing charm quarks.

The formation of a mixed phase indicating the onset of deconfinement leads to a softening of the equation-of-state at a given beam energy [37]. The location of the so called softest point (*i.e.* where the sound velocity exhibits a minimum) may be discovered by measuring carefully the excitation function of the collective flow of particles.

Event-by-event fluctuations are expected to appear when crossing a first order phase transition, and particularly in the vicinity of the critical endpoint. The identification of a critical point would provide direct evidence for the existence and the character of a deconfinement phase transition in strongly interacting matter.

Charm production plays a particular role at FAIR energies, because charmonium, D-mesons and charmed hyperons are created at beam energies close to the kinematical threshold. Therefore, these particles are sensitive probes of the early, high-density stage of the collision (up to 8 times saturation density !). Collective effects contributing to charm production may be visible for the first time. Charm exchange processes may become important, revealing basic properties of charm propagation in a dense baryonic medium. The situation is analogue to strangeness production at SIS18 energies, where 2–3 times saturation density is probed in Au+Au collisions. In order to perform high statistics measurements, the low cross sections for charm production at threshold beam energies (see Fig. 8) has to be compensated by high beam intensities.

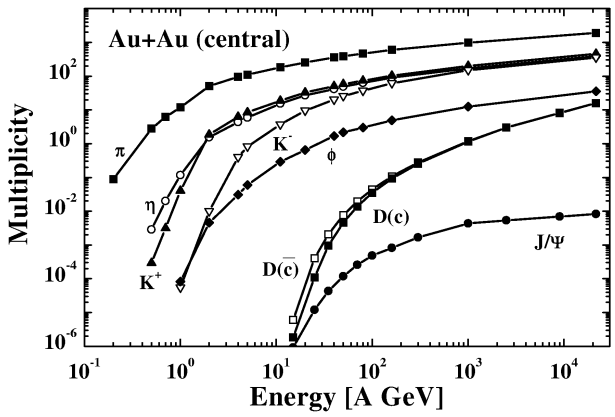

Fig. 8. Multiplicities of mesons produced in central Au+Au collisions as a function of beam energy according to the HSD transport code [38].

3.2. The CBM detector

The experimental task is to identify both hadrons and leptons and to detect rare probes in a heavy ion environment. The apparatus has to measure multiplicities and phase-space distributions of hyperons, light vector mesons, charmonium and open charm (including the identification of protons, pions and kaons) with a large acceptance. The challenge is to filter out those rare probes in Au+Au (or U+U) collisions at reaction rates of up to 10^7 events per second. The charged particle multiplicity is about 1000 per central event. Therefore, the experiment has to fulfill the following requirements: fast and radiation hard detectors, large acceptance, electron and hadron identification, high-resolution secondary vertex determination and a high speed trigger and data acquisition system. The layout of the CBM experimental setup is sketched in Fig. 9.

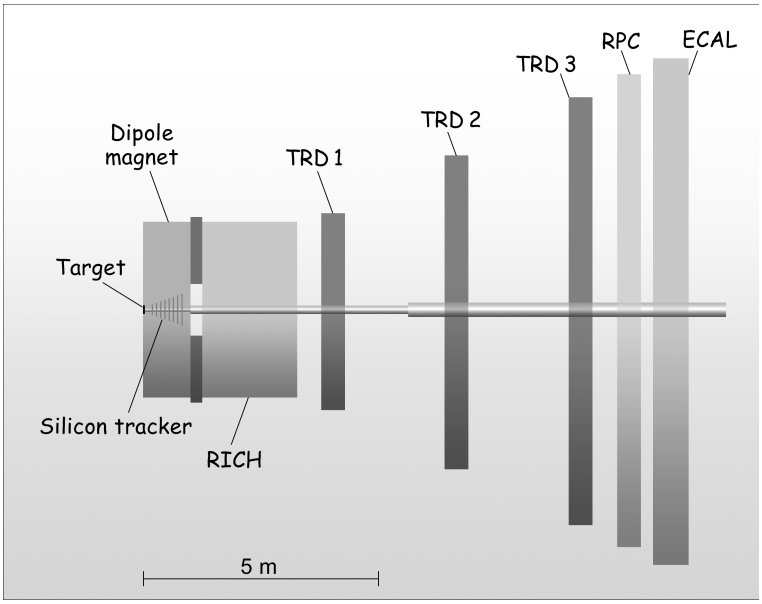

Fig. 9. Sketch of the planned Compressed Baryonic Matter (CBM) experiment. The setup consists of a large acceptance superconducting dipole magnet, radiation-hard Silicon pixel/strip detectors for tracking and vertex determination, Ring Imaging Cherenkov detectors (RICH) and Transition Radiation Detectors (TRD) for electron identification, Resistive Plate Counters (RPC) for time of flight measurement, an Electromagnetic Calorimeter (ECAL) for identification of electrons and photons.

The CBM detector is designed for a comprehensive research program using proton beams (with energies of 10–90 GeV) and nuclear beams (10–45 AGeV) impinging on various targets. The measurements, in particular those of rare diagnostic probes, require a dedicated accelerator with high beam intensities, large duty cycle, excellent beam quality, and with an operational availability of several month per year. Details of the CBM research program and of the setup can be found in the Technical Status report which has been submitted in January 2005 [39]. The CBM Collaboration actually consists of more than 300 persons from 39 institutions and 14 countries.

REFERENCES

[1] F. Wilczek, *Physics Today* **53**, 22 (2000).
[2] F. Weber, *J. Phys. G:, Nucl. Part. Phys.* **27**, 465 (2001).
[3] D. Best *et al., Nucl. Phys.* **A625**, 307 (1997).
[4] Y. Shin *et al., Phys. Rev. Lett.* **81**, 1576 (1998).
[5] F. Laue, C. Sturm *et al., Phys. Rev. Lett.* **82**, 1640 (1999).
[6] P. Crochet *et al., Phys. Lett.* **B486**, 6 (2000).
[7] M. Menzel *et al., Phys. Lett.* **B495**, 26 (2000).
[8] C. Sturm *et al., Phys. Rev. Lett.* **86**, 39 (2001).
[9] A. Förster *et al., Phys. Rev. Lett.* **91**, 152301 (2003).
[10] F. Uhlig *et al., Phys. Rev. Lett.* **95**, 012301 (2005).
[11] J. Aichelin, C.M. Ko, *Phys. Rev. Lett.* **55**, 2661 (1985).
[12] G.Q. Li, C.M. Ko, *Phys. Lett.* **B349**, 405 (1995).
[13] C. Fuchs *et al., Phys. Rev.* **C56**, R606 (1997).
[14] C.M. Ko, G.Q. Li, *J. Phys. G* **22**, 1673 (1996).
[15] W. Cassing, E. Bratkovskaya, *Phys. Rep.* **308**, 65 (1999).
[16] J. Schaffner-Bielich, J. Bondorf, I. Mishustin, *Nucl. Phys.* **A625**, 325 (1997).
[17] C. Fuchs, `nucl-th/0507017`, to be published in *Prog. Part. Nucl. Phys.*
[18] J. Aichelin, *Phys. Rep.* **202**, 233 (1991).
[19] C. Fuchs *et al., Phys. Rev. Lett.* **86**, 1974 (2001).
[20] G.E. Brown *et al., Phys. Rev.* **C43**, 1881 (1991).
[21] G.Q. Li, C.H. Lee, G.E. Brown, *Phys. Rev. Lett.* **79**, 5214 (1997).
[22] T. Waas, N. Kaiser, W. Weise, *Phys. Lett.* **B379**, 34 (1996).
[23] K. Wisniewski *et al., Eur. Phys. J.* **A9**, 515 (2000).
[24] G.Q. Li, C.M. Ko, G.E. Brown, *Phys. Lett.* **B381**, 17 (1996).
[25] Z.S. Wang *et al., Eur. Phys. J.* **A5**, 275 (1999).
[26] A. Larionov, U. Mosel, `nucl-th/0504023`.

[27] C. Hartnack *et al., Eur. Phys. J.* **A1**, 151 (1998).

[28] M.F.M. Lutz, C. Korpa, *Nucl. Phys.* **A700**, 209 (2002).

[29] W. Cassing *et al., Nucl. Phys.* **A727**, 59 (2003).

[30] An International Accelerator Facility for Beams of Ions and Antiprotons, Conceptional Design Report 2001, `http://www.gsi.de/GSI-Future/cdr/`.

[31] M. Stephanov, K. Rajagopal, E. Shuryak, *Phys. Rev.* **D60**, 114028 (1999).

[32] Z. Fodor, S.D. Katz, `hep-lat/0402006`; *J. High Energy Phys.* **0404**, 050 (2004).

[33] S. Ejiri *et al.*, `hep-lat/0312006`.

[34] V.D. Toneev *et al.*, `nucl-th/0309008` and Yu. Ivanov, private communication.

[35] R. Rapp, J. Wambach, *Nucl. Phys.* **A661**, 33c (1999).

[36] C. Blume *et al., J. Phys. G* **31**, 685 (2005); `nucl-ex/0411039`

[37] C.M. Hung, E.V. Shuryak, *Phys. Rev. Lett.* **75**, 4003 (1995).

[38] W. Cassing, E. Bratkovskaya, A. Sibirtsev, *Nucl. Phys.* **A691**, 745 (2001).

[39] CBM Technical Status Report 2005 see: `http://www-linux.gsi.de/hoehne/report/cbmtsr_public.pdf`.